The 2009 IEEE/RSJ International Conference on
Intelligent Robots and Systems
October 11-15, 2009 St. Louis, USA

Leg Mechanisms for Hydraulically Actuated Robots

Yousheng Yang, Claudio Semini, Nikos G. Tsagarakis, Emanuele Guglielmino and Darwin G. Caldwell

Abstract— **The performance of highly dynamic robotic machines is directly associated with both the actuation means and the specific mechanical properties/configuration of the system. Hydraulic actuation demonstrates significant competitive advantages when minimum weight and volume, large forces and wide range of speeds are required and this makes it very suitable for systems such as legged robots. The geometry and design of leg mechanisms have great effect on the actuation system performance such as the required flow, which directly determines the size/weight and power density, in turn affecting the performance of the robot. This paper describes the mechanism and operation principle of two 2-DOF legs considered for HyQ, a hydraulically actuated quadruped robot [1]. Numerical studies have been done to investigate the required flow, the pressure in the actuator chambers and the efficiency of the two leg mechanisms. The results show that the second leg design reduces the required flow significantly with less pressure-jump in the actuator and higher efficiency.**

I. Introduction

Early robotic systems were almost universally hydraulically powered, but in the last decades hydraulic actuation has fallen out of favor in many areas of mechatronics where it is usually replaced by electric drives due to the ease and accuracy of their control. Yet, hydraulic systems remain the most powerful and effective of the actuators available and in comparison to electric actuation, they offer unique advantages, such as high power-to-weight ratio, overload protection and wide range of speed operating conditions. In recent years, hydraulic power has once again seen increased use in robotics with particularly successful applications including the exoskeleton system BLEEX [2], the SARCOS hydraulically actuated humanoid robot CB [3] and the legged robots Kenken II [4], BigDog [5],[6],[7] and COMET-III [8]. The last two robots have four and six legs, respectively, which give them stability to perform exploration and inspection tasks in an outdoor environment. In many cases, they are required to carry heavy loads, with rapid actuation efforts while at the same time they need to be portable, compact and reliable. Considering these requirements, hydraulic actuation seems to be a very promising driving method for legged robots.

Y. S. Yang is with the Italian Institute of Technology, Via Morego 30, 16163 Genoa, Italy (phone: +39-010-71781449; fax: +39-010-720321; e-mail: yousheng.yang@ iit.it).

C. Semini is with the Italian Institute of Technology, Via Morego 30, 16163 Genoa, Italy (e-mail: claudio.semini@iit.it).

N. G. Tsagarakis is with the Italian Institute of Technology, Via Morego 30, 16163 Genoa, Italy (e-mail: nikos.tsagarakis@iit.it).

E. Guglielmino is with the Italian Institute of Technology, Via Morego 30, 16163 Genoa, Italy (e-mail: emanuele.guglielmino@iit.it).

D. G. Caldwell is with the Italian Institute of Technology, Via Morego 30, 16163 Genoa, Italy (e-mail: darwin.caldwell@iit.it).

Due to high nonlinearity, parameter variations and shifting delays [9], most previous studies on hydraulically actuated robots have focused on developing control techniques to address the above issues. Various advanced and sophisticated methods have been proposed improving the tracking control of hydraulically actuated robots including nonlinear feedback control [10],[11], model based adaptive motion control [12],[13] and force/pressure tracking control [14],[15]. However, few researchers have investigated the interaction effects between the robot mechanism and the hydraulic actuation system.

The robot's mechanical design has great effects on the required flow, thus it affects the size of the hydraulic actuation system which in turn affects the power to weight ratio and the system response. If less flow is required in a given hydraulically actuated robot, a smaller pump, lines, valves, and oil supply can be selected, resulting in faster response due to the smaller oil volume and less compressibility. Thus developing a hydraulically-actuated leg, which requires low flow, increases the power-to-weight ratio, reduces the size of the components and the overall weight and improves the system response. In this work, the mechanism, operating principle and advantages/ disadvantages of two different 2-DOF leg designs are presented. The first system is the leg prototype of the quadruped robot HyQ presented in [1] while the second leg design is a revised version of this first leg prototype that is aimed to maximize the performance of the leg mechanism. Numerical studies have been performed to investigate the required flow, the pressure in the actuator chambers and the efficiency of the two leg mechanisms.

The paper is organized as follows: Section II presents the leg mechanisms and their operating principle. Section III introduces the models of the legs and the hydraulic actuation systems. Section IV focuses on the simulation results and the comparison analyses. Finally, section V addresses the conclusions and comments on further development.

II. Leg Mechanisms And Operation Principle

In this research, two leg mechanisms are compared, the first being the original HyQ leg prototype (*leg mechanism A*) and the second a revised and updated leg design (*leg mechanism B*).

A. Leg mechanism A

The mechanism of the first prototype [1], Fig.1, consists of two limb segments (the femur and tibia) and two commercial cylinders and proportional valves. Each of the limb segments has a length of 0.3 m. The leg has two

actuated DOF, both in the sagittal plane: one in the hip and the other in the knee. The range of motion of both joints was determined using data obtained from studies on Labrador Retrievers [16]: both hip/shoulder and knee/elbow flexion/extension joints of the HyQ leg prototype are able to rotate 120°. More details on the design of the leg can be found in [1].

For the frame system shown in Fig.1 (a), the coordinates of the point $P_e(x_e, y_e)$ as a function of the cylinder lengths are given by (1) to (3):

$$x_e = l_1 \sin\varphi_1 - l_2 \sin(\varphi_2 - \varphi_1) \quad (1)$$

$$y_e = l_1 \cos\varphi_1 - l_2 \cos(\varphi_2 - \varphi_1) \quad (2)$$

$$C_i(\varphi_i) = \sqrt{l_{ai}^2 + l_{ai}^2 + 2l_{ai}l_{bi}\cos(\varphi_i + \beta_i - \alpha_i)} \quad (3)$$

where l_{ai}, α_i and β_i are construction parameters set by the desired joint range and maximum stroke, l_{bi} the lever length, $C_i(\varphi_i)$ $(i = 1,2)$ the cylinder length and φ_i the joint angle.

In the first HyQ leg prototype, two 4-way electro-hydraulic proportional valves are used to control the linear actuators. As shown in Fig.2, there are three possible operating modes:

1) $a_1 = a_3 > 0, a_2 = a_4 = 0, \dot{y}_c > 0$, the actuator $C_i(\varphi_i)$ extends, $\varphi_i(i = 1,2)$ decreases.

2) $a_1 = a_3 = a_2 = a_4 = 0$, $\dot{y}_c = 0$, both cylinders come to a standstill if leakage is not taken into consideration. The joint angle φ_i remains unchanged.

3) $a_2 = a_4 > 0, a_1 = a_3 = 0, \dot{y}_c < 0$,, the actuator $C_i(\varphi_i)$ retracts, $\varphi_i$increases.

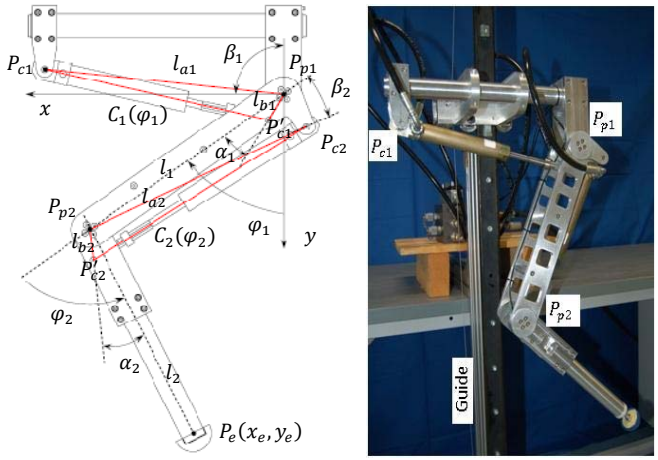

(a) Schematic drawing (b) Photo

Fig.1 The first HyQ leg prototype (Leg mechanism A)

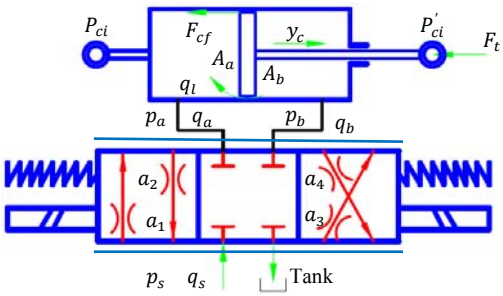

Fig.2 4-way valve-controlled cylinder of leg mechanism A

The parameters defined in Fig.2 are: A_a piston area, A_b piston ring area, $a_i\,(i = 1\sim4)$ flow area of the valve, F_{cf} friction force in the cylinder, F_t load acting on cylinder, p_s supply pressure, p_a pressure in A_a, p_b pressure in A_b, q_s supply flow, q_a the flow to A_a, q_b the flow to A_b, q_l leakage between the piston and cylinder chamber and y_c displacement of piston.

Flow and direction are controlled by the two 4-way electro-hydraulic proportional valves, which also regulate the speed and direction of the cylinders, thus generating the required trajectory.

During walking, running or jumping, the joint angles of human and animal legs usually increase or decrease synchronously i.e. both cylinders move in a linked manner. If leakage is ignored, the flow in the actuation system is:

$$Q_s \geq \sum_{i=1}^{2}\left(\frac{dC_i(\varphi_i)}{dt}A_x\right) = \sum_{i=1}^{2}\left(A_x \frac{l_{ai}l_{bi}\sin(\varphi_i + \beta_i - \alpha_i)}{\sqrt{l_{ai}^2 + l_{ai}^2 + 2l_{ai}l_{bi}\cos(\varphi_i + \beta_i - \alpha_i)}}\frac{d\varphi_i}{dt}\right) \quad (4)$$

where Q_s is the required supply flow of the hydraulic actuation system, A_x is the piston area with $A_x = A_a$ when the cylinder extents and $A_x = A_b$ when the cylinder retracts.

For highly dynamic tasks such as running and jumping a large supply flow is required to drive the actuators. To achieve this high flow, large hydraulic components, which reduce the power density of the system, are needed. One way to reduce the required flow is to consider different mechanical arrangements of the actuator groups. This is the goal in the design of leg mechanism B.

B. Leg mechanism B

The leg mechanism B, Fig.3, also consists of two limb segments and has the same range of motion for both joints. However, Fig.3 and 4 show that the actuation concept is radically different from that of mechanism A.

If the coordinate system is set as shown in Fig.3, the end point $P_e(x_e, y_e)$ of leg mechanism B can be determined by (1),(2) and (5).

$$C_i(\varphi_i) = y_c = r_i\Delta\varphi_i \quad (5)$$

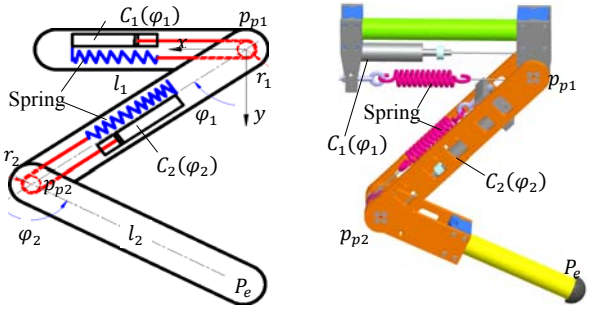

(a) Schematic drawing (b) CAD design

Fig.3. Leg mechanism B

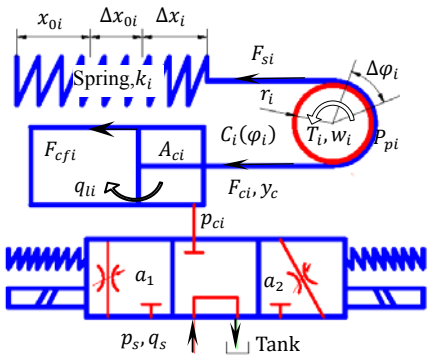

Fig.4 3-way valve-controlled actuator for leg mechanism B

The parameters defined in Fig.4 are: A_{ci} piston ring area, $a_i\,(i = 1{\sim}2)$ flow area of the valve, F_{ci} actuator output force, F_{cfi} friction force in the cylinder, F_{si} spring force, k_i spring constant, p_s supply pressure, p_{ci} pressure in A_{ci}, q_s supply flow, q_{li} leakage in the actuator, r_i radius of joint i, T_i, w_i load and rotary speed of the joint, x_{0i} free length of the spring, Δx_{0i} pre-stretched length of spring, Δx_i stretched length of the spring, φ_i the joint angle and $\Delta\varphi_i$ is the variation of the joint angle φ_i.

Instead of 4-way valves and double acting cylinders, in leg mechanism B, 3-way electro-hydraulic proportional valves are used to control single acting cylinders driving joints by timing belts. There also exist three operation modes, Fig.4:

1) $a_1 > 0, a_2 = 0, \dot{y}_c > 0$, the cylinders retract and stretch the springs. The joint angle φ_1 increases and φ_2 decreases.

2) $a_1 = a_2 = 0,\ \dot{y}_c = 0$, both cylinders remain as they are if leakage is neglected. The joint angle φ_i remains unchanged.

3) $a_2 > 0, a_1 = 0, \dot{y}_c < 0$, under the action of the stretched spring, both cylinders extend. The joint angle φ_1 decreases and φ_2 increases.

When the end point of the leg is moving up and down (as shown in Fig.5), the cylinder for the knee in mechanism B works as a driving cylinder in the first half of the period $(\mathrm{n/f} < t < (\mathrm{n}+0.5)/\mathrm{f})$ retracting under the fluid action and providing the required torque to drive the joint. At the same time it stretches the spring to store energy. In the second half of the cycle$((\mathrm{n}+0.5)/\mathrm{f} < t < (\mathrm{n}+1)/\mathrm{f})$, it performs controlled braking of the joint driven by the stretched spring. Meanwhile, the hip cylinder performs controlled braking of the joint in the first half of the period and drives the knee in the second half. For walking, running or jumping, the actions of the two actuators are similar.

If the leakage is not considered, the required flow of the hydraulic actuation system for leg B can be written as:

$$Q_s \geq \max\left(\sum_{i=1}^{2} \delta_i A_{ci} \frac{dC_i(\varphi_i)}{dt}\right) = \max\left(\sum_{i=1}^{2} \delta_i A_i r_i \frac{d\varphi_i}{dt}\right)\ (i = 1,2) \qquad (6)$$

$$where\ \delta_i = \begin{cases} 0 & actuator\ extending \\ 1 & actuator\ retracting \end{cases}$$

As shown in (6), only the retracting cylinder requires flow. Since the actuators retract asynchronously, the total required flow is reduced significantly.

In general, there are two key differences between the two leg mechanisms, table I.

TABLE I
KEY DIFFERENCES

Name	Leg A	Leg B
Valve	Proportional 4 way	Proportional 3 way
Actuator	Linear actuator	Spring assisted rotary actuator

III. MODELING

In this section the mechanical and hydraulic models of the two leg mechanisms are presented. The models were implemented and analyzed using the LMS Imagine.Lab AMESim[17]. Fig.6 shows the mechanical model and leg kinematics. The two-DOF leg consists of two limb segments (the femur l_1 and tibia l_2) and two joints (hip P_{p1} and knee P_{p2}).

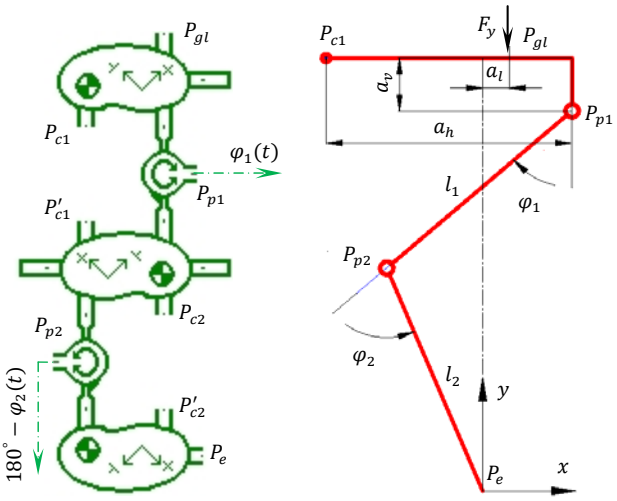

(a) Mechanical model (b) Kinematics definition

Fig.6. Model in AMESim and leg kinematics definition

A. Motion profile for simulation

Two simulations have been performed to investigate the required flow, the pressure in the actuator and the efficiency:

1) In the first scenario (*simulation study 1*) the leg is suspended in the air by hinging connecting point P_{c1} and P_{p1} (called ports in LMS Imagine.Lab AMESim) as shown in Fig.6. The control inputs are the coordinates of the end point of the leg P_e. If the origin of the coordinate system is set

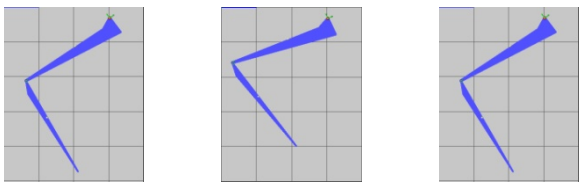

t=*n*/*f* *t*=(*n*+0.5)/*f* *t*=(*n*+1)/*f*

Fig.5. Motion of the end point (*f* is the frequency)

at P_{p1}, the coordinates of P_e, Fig.5, can be expressed as:

$$\begin{bmatrix} x_e \\ y_e \end{bmatrix} = \begin{bmatrix} \cos\varphi_1 & \cos(\varphi_2-\varphi_1) \\ \sin\varphi_1 & \sin(\varphi_1-\varphi_2) \end{bmatrix} \begin{bmatrix} -l_1 \\ -l_2 \end{bmatrix} \quad (7)$$

$$\varphi_i = \varphi_{0i} + A_{mi}\sin(2\pi f_i t + \gamma_i) \quad (8)$$

2) In the second case (*simulation study 2*) the end point P_e is adjacent to the ground link with a revolute pair and the point P_{gl} which is restricted within a vertical guide, only moves vertically with a constant load F_y. If the coordinate system is set up as shown in Fig.6, the motion equation of P_{gl} can be written as:

$$x_{p_{gl}} = a_l, \quad y_{p_{gl}} = y_0 + A_m \sin(2\pi f t) \quad (9)$$

The motion of P_{gl} is shown in Fig.7

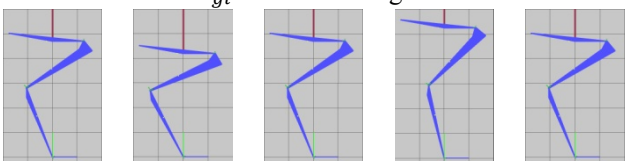

Fig.7. Motion profile for simulation 2 (*f* is the frequency)

The constant load acting on point P_{gl} is:

$$F_x = 0, \; F_y = const. \geq 0, \qquad Torque = 0 \quad (10)$$

B. Model of the hydraulically-actuated leg

Fig.8 and 9 show the model of mechanism A and its electro-hydraulic actuators for simulations 1 and 2, respectively. Fig.9 additionally shows the models of:

1) The closed loop control which contains the control inputs, two proportional valve-controlled actuators and measuring devices (transducers).

2) The power source composed of a gear pump in parallel with a relief valve to control the supply pressure and other hydraulic accessories.

The power source and the measuring devices are the same in both simulations.

For leg mechanism B, the two actuators directly connect to the two revolute pairs P_{p1} and P_{p2} as shown in Fig.6 and the ports P_{c1} and P'_{c1}, P_{c2} and P'_{c2} are free (no force and torque acting on these ports). The power source, the reference input signal and the measuring devices are identical to those used for the model of mechanism A apart from controller gains.

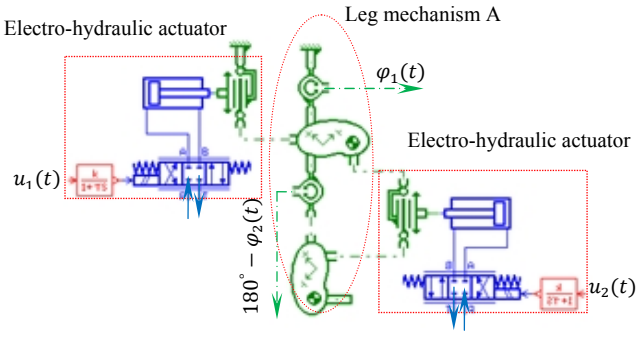

Fig.8. Model of leg mechanism A for simulation 1

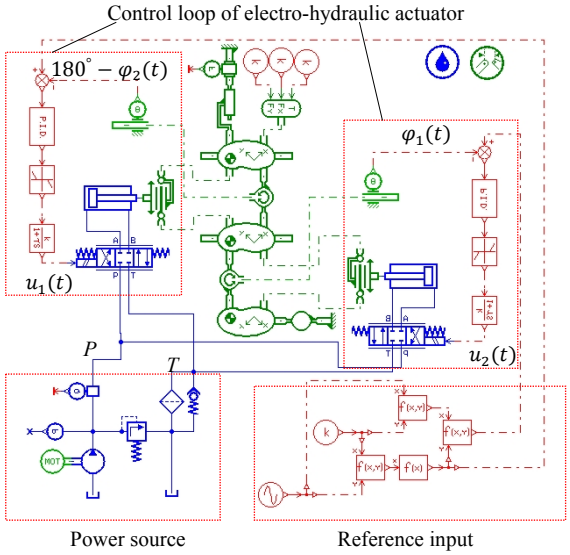

Fig.9. Model of leg mechanism A for simulation 2

C. Parameters

According to the previous study [1], the parameters of the actuators are set as shown in Table II.

TABLE II
KEY ACTUATOR SPECIFICATIONS

Parameter	Value
Cylinder stroke	70 mm
Piston diameter	16 mm
Rod diameter	10 mm
Dead volume at the ends	25 cm^3
Leakage coefficient	0.001 L/min/MPa
Viscous friction coefficient	1 N/(m/s)

For leg mechanism B, the spring constant is 20 kN/m and the pre-stretched length is 20 mm.

The working medium used in the simulations is hydraulic oil of the type ISO VG 46. The specifications of the oil are shown in Table III.

TABLE III
SPECIFICATIONS OF ISO VG 46

Parameter	Value
Density	860 kg/m^3
Bulk modulus	1600 MPa
Absolute viscosity	46 cP
Absolute viscosity of air	0.01934 cP
Max air/gas content	9 %
Temperature	50 ℃

IV. RESULTS AND ANALYSES

A series of simulations have been carried out on the two legs using the models outlined above with a working pressure of 160 bar. The evaluation of the performance of the two leg prototypes was based on the simulation results.

A. Reference trajectory and simulation results

Fig.10 (a) shows the desired position of point P_{gl} in the

second simulation and the numerical results of the two leg mechanisms. It can be seen that there is good agreement between the output trajectory and the desired trajectory with absolute errors <0.005 m, Fig.10 (b). This implies that the desired motion can be generated with a reasonable accuracy by the controllers used in the two leg mechanisms.

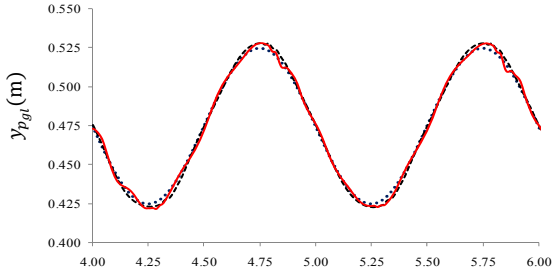

(a) Position of the point P_{gl}

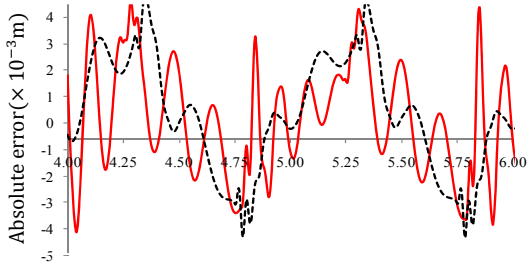

(b) Absolute error

Fig.10. Simulation results of $y_{p_{gl}}$ motion

(··· Desired motion — leg mechanism A, --- leg mechanism B)

B. *Torque acting on the rod of the actuator*

Fig.11 shows the relative rotation of the knee actuators to the corresponding leg segments in mechanism A. It can be seen that the actuators have nonlinear rotational movement, which implies the presence of angular acceleration and torque acting on the actuator. Furthermore, when the actuator extends, a compressive force always acts on the end of the rod. These two cases can make the rod bend or break and the piston incline, thus affecting the performance of the actuator, as deadlock, large leakage and friction force may occur (buckling).

For mechanism B, the actuators rotate synchronously with the corresponding leg segments and there is no relative movement between them. Therefore, there are no radial forces acting on the cylinders. For both cylinder extension and retraction, only tensile force acts on the rods giving a smooth performance.

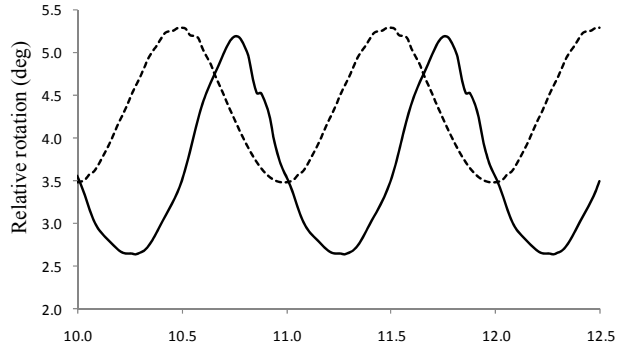

Fig.11. Relative rotation of the actuators for the knee in leg mechanism A

(—simulation 1, --- simulation 2)

C. *Required flow*

According to (4) and (6), the flow is primarily dependent on the motion, the mechanism, the actuators and the control accuracy. Hence, the following conditions should be met for both leg mechanisms:

1) The reference inputs $y_{refi}(t)$ should be the same and the piston diameters should be equal for both legs.

2) The control accuracy achieved by tuning the controller gains should be comparable.

For simulation 1, the reference input for both leg mechanisms is given by (7) and (8), in which $\varphi_{01} = 30^{\circ}$, $\varphi_{02} = 60^{\circ}, A_{mi} = (-1)^{i+1} \times 10^{\circ}$, $\gamma_i = (-1)^{i+1} \times 0.5\pi$, $f_i = 1$ Hz, $l_i = 0.3$m, $a_v = 0.032$m, $a_h = 0.303$ m, Fig.6 (b). For simulation 2, the reference input is given by (9), in which$y_0 = 0.475$ m, $A_m = 0.05$ m, $f = 1$ Hz, $F_y = 100$ N, $a_l = 0$ m. The PID gains have been chosen so that the absolute errors of both simulations were <0.005 m.

Fig.12 depicts the theoretical and numerical results for flow in each leg mechanisms. It can be seen that:

1) For both mechanisms, the numerical results are larger than the theoretical ones and the discrepancy in simulation 1 (Fig.12 (a)) is smaller than in simulation 2 (Fig.12 (b)). The actual required flow does not only depend on the actuator motion, but also on the leakage in hydraulic components, the control error as well as the load. The theoretical one is

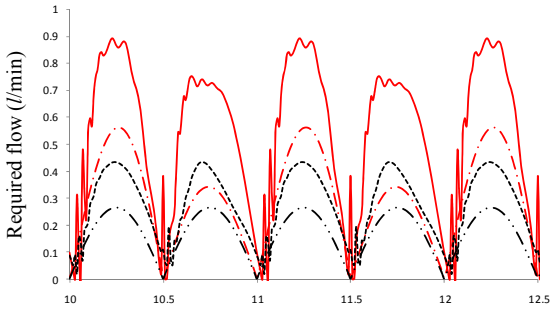

(a) Simulation 1

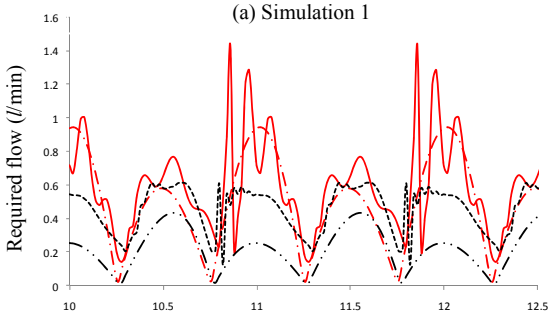

(b) Simulation 2

Fig.12. Required flow

(— Theoretical required flow according to (4)

— Numerical required flow of leg mechanism A

·—Theoretical required flow according to (6)

--- Numerical required flow of leg mechanism B)

calculated only based on the motion, which leads to small values. The load determines the pressure in the actuator chambers, which directly acts on the valve, thus affecting the flow passing through. It needs times to adjust the valve opening width to meet with the motion. This means that there will be a large discrepancy in the required flow if the load change is big. This is why the discrepancy of simulation 2 is larger.

2) The maximum required flow of the leg mechanism A is more than twice larger than that of leg mechanism B for both the theoretical and numerical results, which means that the supply flow of the hydraulic actuation system for leg A should be at least twice that for leg B. Generally, the higher the supply flow, the larger and heavier the actuation system. This simply implies that the power density of leg A is smaller than that of leg B.

3) For both leg mechanisms, the required flows pulse every half second, with the pulses of leg A being larger than those of leg B. This phenomenon is directly related to the pressure pulses. The motion frequency is 1Hz, this means that the direction of the actuators motion reverse every half second. Due to the compressibility of the working medium, pressure pulsation occurs in the actuator when its speed is near to zero, which directly acts on the valve, thus affecting the flow [18]. For leg B, the spring can compensate for these pressure variations giving smaller pressure and flow pulses.

D. Pressure in the actuators' chambers

Fig.13 shows numerical results of the pressure in the actuator chambers. It can be observed that:

1) There are high pressure jumps in the chambers of the actuators for mechanism A even without load. For a symmetric 4-way valve controlled asymmetric-actuator, Fig. 2, the steady pressure in the actuator chambers can be expressed as function of the supply pressure and the load if the leakage and friction force are not taken into consideration (as shown in Table IV).

From Table IV, it can be seen that both the ratio r of the piston area to the piston ring area and the load acting on the actuator have a significant effect on the pressure jump. Using the equations of Table IV, the pressure-jump for p_a is around 50bar and p_b 82bar for simulation 1, which are larger than the numerical results (p_a 35bar, p_b 55bar, Fig.13.(a)) due to the leakage and friction force not being taken into consideration in Table IV.

TABLE IV
PRESSURE IN ACTUATOR CHAMBERS

	p_a	p_b
$\dot{y}_c > 0$ $a_1 = a_3 > 0$ $a_2 = a_4 = 0$	$\left(p_s + \frac{F_t}{A_a} r^3\right)\frac{1}{1+r^3}$	$\left(p_s - \frac{F_t}{A_a}\right)\frac{r}{1+r^3}$
$\dot{y}_c < 0$ $a_2 = a_4 > 0$ $a_1 = a_3 = 0$	$\left(p_s - \frac{F_t}{A_b}\right)\frac{r^2}{1+r^3}$	$\left(r^3 p_s + \frac{F_t}{A_b}\right)\frac{1}{1+r^3}$

where p_s is the system supply pressure, F_t is the load for the actuator, $r = A_a/A_b$, $\dot{y}$ is the actuator speed.

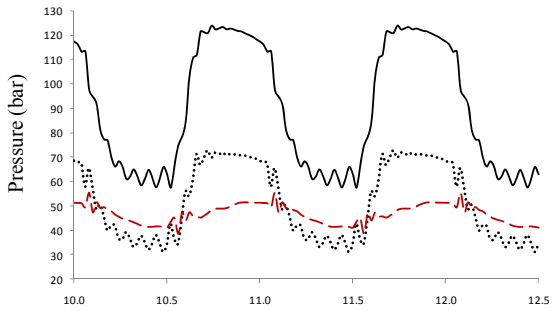

(a) The actuators for the hip in simulation 1

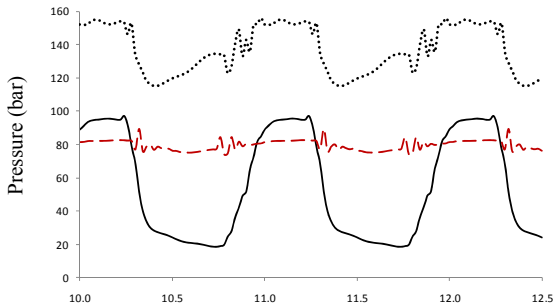

(b) The actuators for the knee in simulation 2

Fig.13. Pressure in actuator chambers
(— Pressure in the chamber with rod for leg mechanism A
···· Pressure in the chamber without rod for leg mechanism A
--- Pressure in the chamber for leg mechanism B)

2) There is little pressure pulsation when the actuator is reversing direction in leg B. If the friction force is neglected, the steady pressure in the actuators for mechanism B is:

$$p_{ci} = \frac{k_i(\Delta x_{0i} + \Delta x_i)}{A_{ci}} + \frac{T_i}{r_i} \tag{11}$$

From (11), the steady pressure in the actuators for leg B is determined by the load and spring constant. The small pressure ripple is caused by the compressibility of the working medium.

E. Efficiency

The efficiencies of the two legs are compared in simulation study 2, with efficiency defined as:

$$\eta = \frac{\int_{t_0}^{t_0+nT} \left| F_{gl} \cdot v_{gl} \right| dt}{\int_{t_0}^{t_0+nT} \left| p_s \cdot Q_r \right| dt} \tag{12}$$

where T is the period, $F_{gl}$the force acting at point P_{gl}, v_{gl} the velocity of P_{gl}, p_s the supply pressure and Q_r the required flow as shown in Fig.12.

The efficiency vs. time plot for the two leg mechanisms, Fig.14, shows that the efficiency for both leg mechanisms approaches a constant, with the efficiency of leg B being a little higher (around 2%) than that of leg A. This can be attributed to the energy loss (flow through an orifice) in the control valves. In mechanism A, where two four-way-valves are used to control two actuators, there are four orifices (two from the *p* port to the actuators, two from the actuators to the tank), while for mechanism B, there are just two orifices

working at the same time. This implies that the energy loss in the valves for leg A is larger than that for leg B, giving leg B the higher efficiency.

The efficiency shown in Fig.14 does not include the effects of the relief valve in the power system as shown in Fig.9. In actual hydraulic actuation systems, the supply flow should be not less than the maximal required flow if there is no other auxiliary power source such as an accumulator. According to the flow analysis in IV.C, a smaller pump with significantly less flow is sufficient for leg mechanism B and therefore its total efficiency is approximately twice that of mechanism A, for a given load performing the same motion under the same supply pressure.

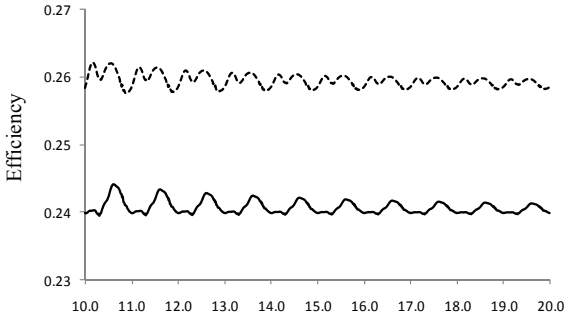

Fig.14. Efficiency for the two leg mechanisms
(— leg mechanism A ---leg mechanism B)

V. Conclusion and Future Work

In this work, two 2-DOF hydraulically-actuated leg mechanisms were presented and evaluated through simulation studies. Theoretical and numerical studies have been done to investigate the effects of leg mechanisms on the hydraulic actuation system. Comparison analyses were also made on the theoretical and numerical results of the two leg mechanisms, Table V.

TABLE V
Main Effects On Hydraulic Actuation System

Name	Leg A	Leg B
Required flow	Large	Small
Efficiency	Low	High
Risk of buckling	Yes	No
Pressure jump	Big	Small

Several conclusions can be drawn as follows:

1) The mechanical design of a robot leg has a great influence on the power required in an actuation system, and good design can reduce the demands on the actuation system as well as improving the overall performance.

2) For a hydraulically-actuated multi-DOF leg, the required flow can be reduced by making the cylinders work alternately and using springs as power storage for a reciprocal motion.

3) Using a symmetrical valve to control an asymmetrical actuator will cause pressure jumps in the actuator chambers. So it is better to use an asymmetrical valve to control an asymmetrical actuator or a symmetrical valve with a symmetrical actuator.

Future work will include the following:

1) Prototyping of one leg actuated by the 3-way valve controlled hydraulic actuator, as shown in Fig.3.

2) Experimental tests to evaluate the leg performance in terms of required flow, dynamic response, efficiency and load capacity under different pressures and with different springs and to compare them with the simulation results.

3) Optimization of the leg design based on the experimental and numerical findings.

References

[1] C. Semini, N. G. Tsagarakis, B. Vanderborght, Y. Yang and D. G. Caldwell, "HyQ – Hydraulically Actuated Quadruped Robot: Hopping Leg Prototype," IEEE/RAS Int. Conf. on Biomedical Robotics and Biomechatronics (Biorob), pp.593-599, 2008.

[2] Zoss, A. B., Kazerooni, H. and Chu A., 2006, "Biomechanical design of the Berkeley lower extremity exoskeleton [BLEEX],"IEEE/ASME Transactions on Mechatronics, 11[2], pp.128-138.

[3] Sang-Ho, H., Hale, J. G., Cheng, G., 2007, "Full-Body Compliant Human–Humanoid Interaction: Balancing in the Presence of Unknown External Forces", IEEE Transactions on Robotics and Automation, 23[5], pp. 884 – 898.

[4] S. Hyon, S. Abe, and T. Emura, "Development of a biologically inspired biped robot KenkenII," in Japan-France Congress on Mechatronics & 4th Asia Europe Congress on Mechatronics, pp. 404-409, Sept.2003.

[5] R Playter, M Buehler, and M. Raibert, "BigDog," Proceedings of SPIE 6230, pp. 896-901, April 2006.

[6] M. Buehler, R. Playter, and M. Raibert, "Robots Step Outside," Int. Symp. Adaptive Motion of Animals and Machines [AMAM], Ilmenau, Germany, Sept 2005.

[7] M. Raibert, K. Blankespoor, G. Nelson, R. Playter and the Bigdog Team, "BigDog, the Rough-Terrain Quadruped Robot," Proceeding of the 17th IFAC World Congress, pp.10822-10825, 2008.

[8] R.K.Barai, and K.Nonami, "Locomotion control of a hydraulically actuated hexapod robot by robust adaptive fuzzy control with self-tuned adaptation gain and dead zone fuzzy pre-compensation," J. Intelligent and Robotic Systems, 55[1] , pp.35-66. 2008

[9] N.D.Manring, 2005, "Hydraulic control systems," John Wiley&Sons, Inc, New Jersey.

[10] M.R.Sirouspour and S.E.Salcudean, 2001, "Nonlinear control of Hydraulic Robots," IEEE Trans. Rob. Autom., 17(2), pp.173-182.

[11] B.Yao, F. Bu, J. Reedy and G.T.-C. Chiu, "Adaptive robust motion control of single-rod hydraulic actuators: theory and experiments," IEEE/ASME Trans. Mechatronics, 5(1), pp.79-91, 2000.

[12] T.C.Tsao and M.Tomizuka, "Robust adaptive and repetitive digital control and application to hydraulic servo for noncircular machining," *ASME* J. Dyn. Syst., Meas. Control, Vol.116, pp.24-32, 1994.

[13] M. Honegger and P.Corke, "Model-based control of hydraulically actuated manipulators," Proceedings of the IEEE Int. Conf. on Robotics and Automation, pp.2553-2559, 2001.

[14] R.Liu and A. Alleyne, "Nonlinear Force/Pressure Tracking of an Electro-Hydraulic Actuator," ASME J. Dyn. Syst., Meas. Control, Vol.121, pp.232-237, 2000.

[15] W.H.Zhu and J.C.Piedboeut, "Adaptive output force tracking control of hydraulic cylinders with applications to robot manipulators," J.Dyn.Syst. Meas. Control, Vol.127, pp.206-217, 2005.

[16] G. Jaegger, D. Marcellin-Little and D. Levine, "Reliability of Goniometry in Labrador Retrievers," AJVR, vol. 63, No. 7, pp. 979-986, July 2002.

[17] LMS Imagine.Lab AMESim, http://www.lmsintl.com/imagine-amesim-intro.

[18] D. McLoy and H. R. Martin "*Control of fluid power: analysis and design*," Wiley, 1980.